

Structural origins of the low-temperature orthorhombic to low-temperature tetragonal phase transition in high- T_c cuprates

Jeremiah P. Tidey ¹, Christopher Keegan ², Nicholas C. Bristowe ³, Arash A. Mostofi ², Zih-Mei Hong ^{4,5},
Bo-Hao Chen ⁶, Yu-Chun Chuang ⁶, Wei-Tin Chen ^{4,7} and Mark S. Senn ^{1,*}

¹Department of Chemistry, University of Warwick, Gibbet Hill, Coventry CV4 7AL, United Kingdom

²Departments of Physics and Materials, and the Thomas Young Centre, Imperial College London, London SW7 2AZ, United Kingdom

³Centre for Materials Physics, Durham University, South Road, Durham DH1 3LE, United Kingdom

⁴Center for Condensed Matter Sciences and Center of Atomic Initiative for New Materials, National Taiwan University, Taipei 10617, Taiwan

⁵Department of Chemistry, Fu-Jen Catholic University, New Taipei 24205, Taiwan

⁶National Synchrotron Radiation Research Center, Hsinchu 30076, Taiwan

⁷Taiwan Consortium of Emergent Crystalline Materials, Ministry of Science and Technology, Taipei 10622, Taiwan



(Received 25 November 2021; revised 24 June 2022; accepted 6 July 2022; published 8 August 2022)

We undertake a detailed high-resolution diffraction study of a plain band insulator, La_2MgO_4 , which may be viewed as a structural surrogate system of the undoped end-member of the high- T_c superconductor family $\text{La}_{2-x-y}\text{A}_x^{2+}\text{R}_y^{3+}\text{CuO}_4$ ($\text{A} = \text{Ba}, \text{Sr}$; $\text{R} = \text{rare earth}$). We find that La_2MgO_4 exhibits the infamous low-temperature orthorhombic (LTO) to low-temperature tetragonal (LTT) phase transition that has been linked to the suppression of superconductivity in a variety of underdoped cuprates, including the well-known $\text{La}_{2-x}\text{Ba}_x\text{CuO}_4$ ($x = 0.125$). Furthermore, we find that the LTO-to-LTT phase transition in La_2MgO_4 occurs for an octahedral tilt angle in the 4° – 5° range, similar to that which has previously been identified as a critical tipping point for superconductivity in these systems. We show that this phase transition, occurring in a system lacking spin correlations and competing electronic states such as charge density waves and superconductivity, can be understood by simply navigating the density functional theory ground-state energy landscape as a function of the order parameter amplitude. This result calls for a careful reinvestigation of the origins of the phase transitions in high- T_c superconductors based on the hole-doped, $n = 1$ Ruddlesden-Popper lanthanum cuprates.

DOI: [10.1103/PhysRevB.106.085112](https://doi.org/10.1103/PhysRevB.106.085112)

I. INTRODUCTION

High-temperature superconductors based on $\text{La}_{2-x}\text{Ba}_x\text{CuO}_4$ (LBCO), in which unconventional superconductivity was first reported [1], continue to receive significant attention for their intertwined electronic orders and promise of insights towards room-temperature superconductivity (SC) [2–4]. Nevertheless, a comprehensive understanding of the origin and mechanism behind such phenomena remains elusive [5]. While significant efforts have recently been made to explain the interplay of their competing electronic states [6,7], these fall short of reconciliation with the complex structural behavior concurrently observed [8].

The doping-dependent temperature phase diagram of the canonical system, LBCO, exhibits two pronounced regions of superconductivity, with peaks in the critical transition temperature for superconductivity, T_c , at $x = 0.095$ and 0.155 , on either side of a pronounced dip for $x \sim \frac{1}{8}$ doping [9]. This suppression of T_c is understood to be coincident [10] with

a structural phase transition, commencing below 80 K (T_{LT}) from the low-temperature orthorhombic (LTO) phase ($Bmab$) to a low-temperature tetragonal (LTT) phase ($P4_2/nm$) [11]. This phase transition has been linked to the emergence of a charge density wave (CDW) state [12] that is thought to compete with three-dimensional superconductivity [13–15]. Since the LTT phase itself is not observed in the undoped end-member, La_2CuO_4 , and appears otherwise to be localized in the temperature, doping, and composition phase diagram at points coincidental with suppression of T_c [11,16,17], it has often been assumed that this phase arises as a result of an interplay between electronic, spin, and lattice degrees of freedom near $x \sim \frac{1}{8}$ chemical doping [18,19]. However, the contrary position, that the electronic ordering in cuprates is sensitive to the structural order and not the other way around, has also been discussed [11,20]. It is evident, therefore, that consensus on the important and contentious issue of the origin of these transitions has not yet been reached.

A great deal of work has been done towards accurately elucidating the structure-property relationships in this class of materials [21]. This has yielded a few simple connections: for example, that the structural transitions occur in response to mismatch of the La-O and Cu-O bond lengths [22] and that a greater difference between La and the R dopant favors the LTT phase [23] (see below). However, these are all drawn as observations from electronically complex materials where this convolution serves to obfuscate a clear disentangling of

*m.senn@warwick.ac.uk

electronic and structural contributions to those phase transitions. A notable example for this paper is that, while it is understood that a higher variance in the size of the *A*-site cation stabilizes the LTT phase [21], lower variance is also linked to stabilizing superconductivity [24], which will itself impart a contribution to the total energy landscape. To properly resolve the structure-property relationships in these materials, the specific contributions need to be precisely and individually understood.

To make progress in understanding any entanglement between structural symmetries, superconductivity, and charge density waves, it is important to understand the precise symmetries and structural mechanisms implicated in their behavior. Indeed, even in the undoped end-member, La_2CuO_4 , the true structure and its physical origin remain a topic of discussion [25–27], where observations of low-temperature less-orthorhombic (LTLO) or even monoclinic distortions to the LTO structure have been assessed. To gain insight into this question, we synthesize a surrogate of the end-member, La_2MgO_4 . Charge balance is here achieved with all atoms adopting low-energy, closed-shell electronic configurations and, thus, it is reasonable to infer that the structural behavior be void of electronic ordering contributions.

II. EXPERIMENTAL DETAILS

Polycrystalline La_2MgO_4 was prepared via high-pressure synthesis from stoichiometric amounts of La_2O_3 (Alfa Aesar, 99.999%, dried by heating at 1273 K for 12 h) and MgO (Acros, 99.99%). The starting materials were mixed thoroughly, sealed in a gold capsule, and heated at 1273 K at 6 GPa for 30 min in a DIA-type cubic anvil high-pressure apparatus. The sample was quenched to room temperature after the heating program, and the pressure was released slowly. La_2MgO_4 adopts a Ruddlesden-Popper (RP) $n = 1$ structure consisting of single MgO_6 perovskite slabs separated by LaO rocksalt layers (Fig. 1). As Mg^{2+} has almost the same ionic radius as Cu^{2+} (0.72 vs 0.73 Å, respectively) [28], it may be viewed as a structural surrogate to the end-member of the RP $n = 1$ superconducting cuprate La_2CuO_4 , but with the key difference being that it necessarily lacks the electron-electron correlations from which competing emergent phenomena may arise.

To ascertain the temperature-dependent structural phase diagram, synchrotron x-ray powder diffraction measurements were conducted on beamline 19A of the Taiwan Photon Source, National Synchrotron Radiation Research Center (TPS, NSRRC), with a 20- and 16-keV incident beam ($\lambda = 0.61994$ Å and $\lambda = 0.77495$ Å) for the low- and high-temperature sweeps, respectively, using a microstrip system for time-resolved experiments (MYTHEN) detector. The La_2MgO_4 sample was sealed in a 0.1-mm borosilicate capillary for low temperature and 0.1-mm quartz capillary for high-temperature experiments, each kept spinning during data collection for better powder averaging. A Cryostream 800 Plus (Oxford Cryosystems) was utilized for data collection from 100 to 450 K with intervals of 50 K (omitting 400 K). A hot air gas blower (FMB Oxford) was utilized for data collection from 300 to 1000 K, at intervals of 10 K from 300 to 370 K, 50 K from 400 to 500 K, and 10 K from

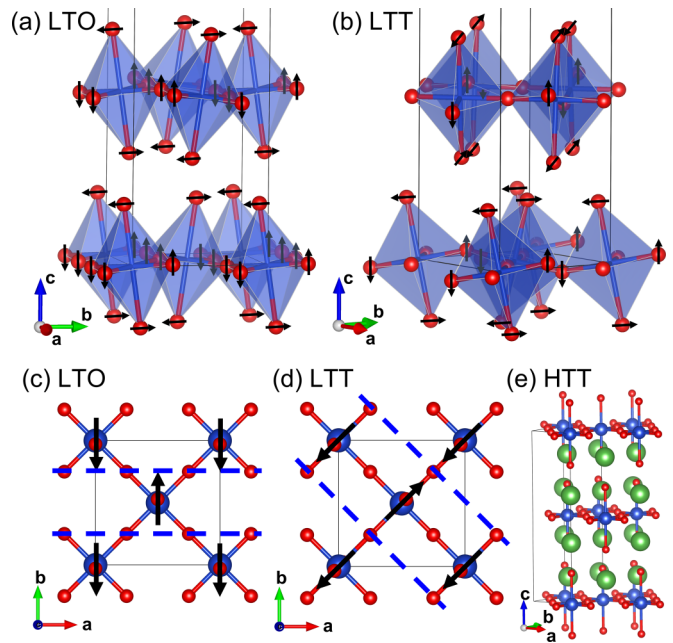


FIG. 1. (a) and (b) Off-axis representations of the two unique planes and (c) and (d) views along the *c* axis of the basal planes of the LTO and LTT structures common to the lanthanum cuprates and shared by La_2MgO_4 , showing the sense of the BO_6 octahedral tilts and excluding *A*-site cations for clarity. The arrows indicate the displacement of visible [(a) and (b)] and apical [(c) and (d)] oxygen atoms with the buckles to the BO_2 planes further illustrated. (e) High-temperature tetragonal (HTT) phase with untitled octahedra with the positions of the *A*-site (La, etc.) ions indicated (green spheres). *B*-site (Mg, Cu, etc.) and oxygen atoms are depicted in blue and red, respectively.

510 to 1000 K. All measurements were taken upon warming. Rietveld refinement of the data was performed in TOPAS 6 [29] using the symmetry-adapted displacement formalism [30], as implemented in ISODISTORT [31]. All refinements were performed in the $(\mathbf{a} + \mathbf{b}, \mathbf{a} - \mathbf{b}, \mathbf{c})$ supercell with respect to the $I4/mmm$, high-temperature tetragonal (HTT) aristotype phase, and in the common subgroup $Pccn$ with appropriate constraints imposed on the symmetry-adapted displacements and lattice parameters to reproduce the symmetry of the HTT ($F4/mmm$ in the aforementioned supercell), LTO, or LTT phase. For each phase, the scale factor, isotropic thermal displacement parameters (for each atom type), Stephens strain parameters [32], and atomic positions as described above were fitted, along with impurity phases as detailed in the Supplemental Material (SM; see Ref. [33]) [10,29–32,34–40]. For the temperature range 300–340 K of the high-temperature sweep, we observed clear phase coexistence of the LTO and LTT phases (Fig. 2), although a model reliable enough for structural discussion could not be obtained until 370 K. Further details and representative fits are given in the SM.

III. RESULTS AND DISCUSSION

For temperatures above 950 K, the aristotypical $n = 1$ RP symmetry is observed with space group $F4/mmm$ in the

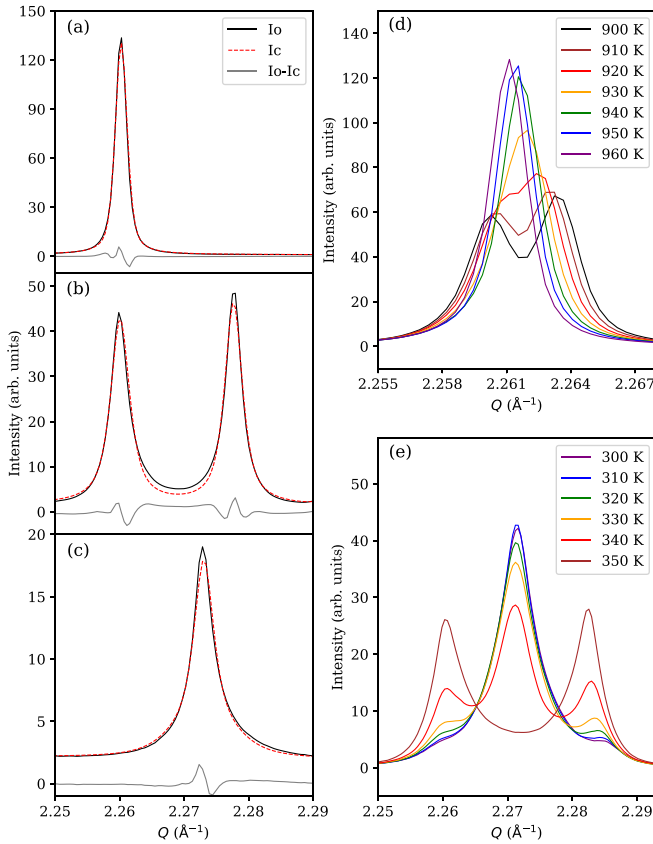


FIG. 2. A plot of the Rietveld fit to the (a) $(110)_{\text{HTT}}$ diffraction profile, which becomes (b) $(200)_{\text{LTO}}$ or $(020)_{\text{LTO}}$ and, further, (c) $(200)_{\text{LTT}}$, shown at 990, 500, and 100 K, respectively. In all cases a single-phase model is used to fit the data. (d) and (e) show the evolution of peak profiles across the LTO-to-HTT and LTT-to-LTO phase transitions, evidencing second- and first-order behavior, respectively.

supercell setting, with any splitting of the (200) diffraction profile clearly absent [Fig. 2(a)]. Below 950 K, a second-order phase transition occurs, evidenced by a continuous evolution of the lattice parameters (Fig. 3). This phase is well fit by the $Bmab$ (LTO) phase (Fig. 1) that is typically taken to be the ground-state structure of undoped La_2CuO_4 [41]. The diffraction profile of the (200) peak shows a continuous splitting into well-resolved (200) and (020) reflections. This phase transition may be described as an out-of-phase rotation of the MgO_6 octahedra about \mathbf{a} axis. Following the conventions of ISODISTORT [31], the order parameter (OP) associated with this tilting may be labeled as transforming as the irreducible representation (irrep) $X_3^+(a;0)$, while the tilt system of the perovskite slabs can be labeled in Glazer notation as $\mathbf{a}^-\mathbf{a}^-\mathbf{c}^0$ with respect to the lattice vectors of the aristotypical HTT cell.

Below 350 K, a third distinct phase is observed with tetragonal symmetry and fitting well to the LTT phase that has been much discussed in the underdoped cuprates, most notably in LBCO ($x \sim \frac{1}{8}$). This corresponds now to alternating tilting of the octahedra about the $[110]$ and $[1\bar{1}0]$ axes in the perovskite layers, centered at z and $z + \frac{1}{2}$, and may be described by an OP transforming as the irrep $X_3^+(a;a)$ ($\mathbf{a}^-\mathbf{a}^0\mathbf{c}^0$). We note

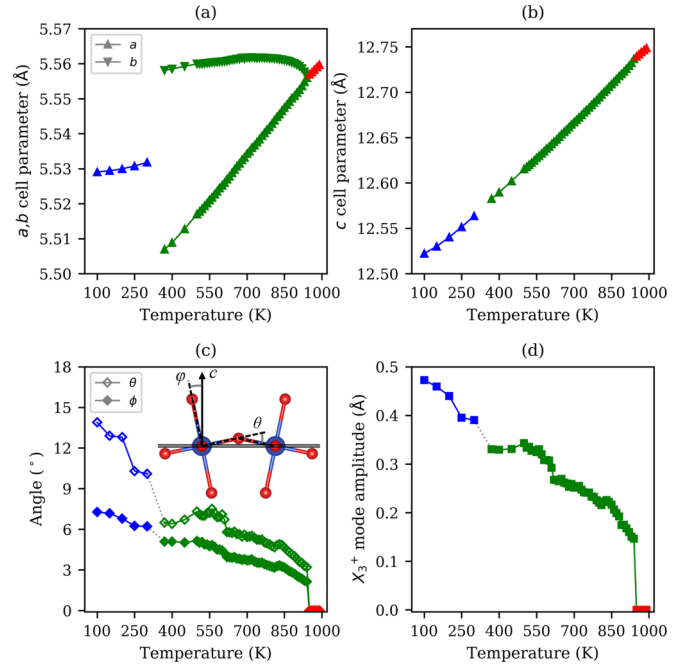


FIG. 3. Parameters extracted by Rietveld refinement against variable-temperature powder diffraction data collected on La_2MgO_4 . Colors denote LTT (blue), LTO (green), and HTT ($F4/mmm$ setting; red) single-phase regimes. HTT cell parameters are reported in the supercell setting for clarity. Angles of the octahedral tilt and Mg-O-Mg buckle are determined from the refined atomic positions. The X_3^+ OP mode amplitude is the total mode amplitude A_p value as defined by ISODISTORT [31]. A discussion of the errors in this plot can be found in the SM.

that this occurs at a temperature much higher than in the lanthanum cuprates and speculate that this is due to the lack of Jahn-Teller distortion in the Mg compound compared with the cuprate. This will affect the rumpling at the interface of the perovskite and rocksalt layers, in turn affecting the mismatch between the M -O bonds (mentioned above). Discussion of this is beyond the scope of this paper and will be the subject of a future large body of work.

Upon warming through this transition, a clear coexistence between the LTT and LTO phases is observed [Fig. 2(e)]. Along with the discontinuous jump in the lattice parameters and refined magnitude of the OP (Fig. 3), this behavior is typical of the first-order nature of the phase transition that is expected in the absence of a group-subgroup relationship between the two phases and replicated throughout the doped lanthanum cuprates, for which the sample is a surrogate. Further justification for using La_2MgO_4 as a surrogate system in our investigations of the origins of the soft-mode phase transition in lanthanum cuprates is provided by a comparison of various crystallographic and structural parameters in the SM [33]. Since this phase transition has invariably been found to be concomitant with the suppression of superconductivity and the formation of CDWs, the observation of the LTT phase in a system that is a plain band insulator, i.e., lacking the possibility of strong electronic correlations, allows an opportunity for clear insight into the structural contributions to the

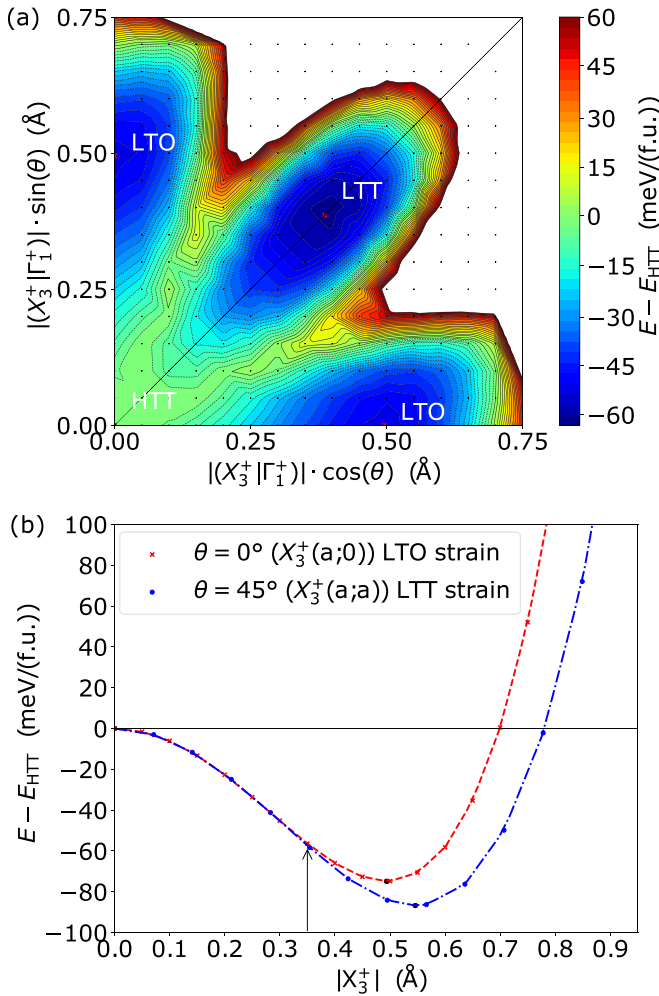


FIG. 4. (a) The energy landscape for a given direction and magnitude of the $X_3^+(a;b)$ OP with simultaneous interpolation of the Γ_1^+ OP and strain field between the HTT, relaxed LTO, and relaxed LTT phases, calculated relative to the nonstandard, $F4/mmm$, HTT phase (see SM for further details). (b) Plot of the energy landscape along the $X_3^+(a;0)$ and $X_3^+(a;a)$ OP directions at the calculated relaxed values of strain and Γ_1^+ OP for the LTO and LTT phases, respectively, relative to the HTT aristotype (see SM). All mode amplitudes given are A_p values as defined by ISODISTORT [31]. The black data points denote the positions of the lowest-energy structures along each OP direction.

mechanism of the LTO-to-LTT phase transition, isolated from the influences of competing electronic phenomena.

To obtain further insight into the origin of the LTO-to-LTT phase transition in La_2MgO_4 , we perform single-point energy calculations using density functional theory (DFT) to map out an energy landscape spanning the $X_3^+(a;0)$ and $X_3^+(a;a)$ OPs. The symmetry in all cases can be described within the $Pccn$ space group, which is a common subgroup of both the LTT and LTO phases and encompasses intermediate-tilt propagation vectors that describe the so-called low-temperature less-orthorhombic (LTLO) structure. Figure 4(a) shows the energy landscape associated with an interpolation of the strain, the X_3^+ OP magnitude and direction, and the Γ_1^+ OP magnitude between the relaxed HTT, LTO, and LTT phases

(see SM). While our results are qualitatively similar to earlier calculations performed on La_2CuO_4 [20], those earlier results neglect spin polarization and electron-electron correlations that need not be modeled in our surrogate system. We note that the reported energy differences between the LTT and LTO phases are small and would be expected to change if spin polarization and electron-electron correlations were modeled. Furthermore, it has been pointed out [10] that these calculations may overestimate the experimentally observed octahedral tilting angles. It is thus hard to justify that such a study could provide concrete proof of the structural origin of the LTO-LTT phase transitions in the cuprates.

Our single-point energy calculations reveal no metastable, local minima for any intermediate $Pccn$ phases between the LTO and LTT structures. This is further supported by full structural relaxations of intermediate $Pccn$ structures which invariably relax to the LTT structure. Since the $Pccn$ phase has lower symmetry than the LTO and LTT phases, we would equally expect its vibrational entropy to be lower. The lower entropy of this phase also makes a stable $Pccn$ phase unexpected with increasing temperature. The LTO-to-LTT phase transition can then not occur via a continuous rotation of the OP that passes through the $Pccn$ phase, meaning it must be first order. This is consistent with the first-order nature of the phase transition evidenced experimentally [i.e., the pronounced phase coexistence; Fig. 2(e)].

While our DFT calculations do not explicitly capture the effect of temperature, we may still gain valuable insights into the sequence of phase transitions in La_2MgO_4 . Figure 4(b) shows the energy landscape with respect to the magnitude of the X_3^+ OP along the (a;0) and (a;a) OP directions for strain and Γ_1^+ magnitudes fixed at the calculated relaxed structures for LTO and LTT, respectively. This reveals that there is a clear departure of the LTO and LTT phases from the harmonic approximation (which requires that all OP directions be isoenergetic) at an amplitude of around $A_p = 0.35$ Å. Such an amplitude lies within the discontinuous region between the LTO and LTT phases, at around 300–350 K in our diffraction study [Fig. 3(d)].

The origin of the experimentally observed LTT-to-LTO phase transition in La_2MgO_4 may then be understood within the quasiharmonic approximation in which the thermal lattice expansion renormalizes the OP amplitude, as we have found in our previous work on RP $n = 1$ systems in which we included the effects of thermal expansion [42]. The increase in amplitude of the OP upon cooling leads to a scenario where the LTT structure becomes more favorable from an enthalpic perspective. Any entropic contributions to the Gibbs free energy that favor LTO at higher temperatures are evidently then quickly overwhelmed. The observation of such a crossover between LTO and LTT superstructures in our surrogate system at a tilt angle between 4° and 5° may indicate why a similar value has been identified as a critical octahedral tilt angle for superconductivity in the family of compounds $\text{La}_{2-x-y}\text{A}_x^{2+}\text{R}_y^{3+}\text{CuO}_4$ ($A = \text{Ba, Sr; R} = \text{rare earth}$) [21], where superconductivity is presumed to be the preserve of the LTO phase.

Finally, we turn our attention to La_2CuO_4 , where we employ DFT with an on-site Hubbard U on the Cu site of 9 eV (see SM), an approach which has been demonstrated

to be effective in approximating the electronic ground state of La_2CuO_4 [43,44]. While our DFT+ U calculations for La_2MgO_4 find the LTT phase to be lower in energy than the LTO phase by ~ 11.2 meV/f.u., for La_2CuO_4 this energy difference is of the order of the typical accuracy of DFT. Prior calculations on La_2CuO_4 using the strongly constrained and appropriately normed (SCAN) exchange-correlation functional also found the two phases to be very close in energy [45]. Earlier calculations investigating the energy landscape of the tilt mode in La_2CuO_4 using fixed lattice parameters taken from experimental structures also found similar energy differences [20].

These results are consistent with the experimental observations that the LTO-to-LTT phase transition is not observed upon cooling for La_2CuO_4 [25–27,41] but is evidenced here as occurring at significantly elevated temperatures in La_2MgO_4 . The small energy scale associated with variation in the ionic radii and changes in spin and electron correlations that occur as the La_2CuO_4 system is doped towards $x = \frac{1}{8}$ may be sufficient to affect small changes in the amplitude of the X_3^+ OP, in turn triggering or indeed inhibiting the transition from LTO to LTT in these systems. This resulting change in structural symmetry is what has often been correlated with the suppression of superconductivity in these systems.

In conclusion, we have shown that the infamous low-temperature tetragonal (LTT) to low-temperature orthorhombic (LTO) phase transition, observed in many underdoped lanthanum cuprates, may be reproduced in the surrogate plain band insulator, La_2MgO_4 , which is presumably devoid of electron-electron correlation inherent to the competing superconducting and CDW states. The transition is shown to be triggered simply by the change in order parameter magnitude associated with the tilt of the BO_6 octahedra ($B = \text{Mg}$ or Cu).

In the doped La_2CuO_4 , small changes in magnetic and electronic correlations (experimentally or *in silico*) will couple to the order parameter magnitude, consequently selecting either LTO or LTT as the ground state, which presumably themselves favor superconductivity or CDW formation, respectively. It is noteworthy that the tilt angle at the relevant OP magnitude lies close to the critical value of tilting that has been associated with the suppression of superconductivity in the doped lanthanum cuprates. It may be further illuminating to investigate how the phase behavior in these electronically simple phases responds to external stimuli, such as a strain field which could be achieved by the formation of epitaxial films.

The diffraction data used in this paper, along with crystallographic information files of the experimental and DFT optimized structures, are available as supporting data sets [46].

ACKNOWLEDGMENTS

This work was partly supported by the Ministry of Science and Technology (Taiwan) (MOST-108-2112-M-002-025-MY3) and Academia Sinica Project No. AS-iMATE-109-13. The synchrotron experiment was supported by the National Synchrotron Radiation Research Center (NSRRC, Taiwan), with Proposal No. 2021-1-024. J.P.T. was funded by EPSRC Grant No. EP/S027106/1. M.S.S. acknowledges support from a Royal Society fellowship (UF160265). C.K. was supported through a studentship in the Centre for Doctoral Training on Theory and Simulation of Materials at Imperial College London funded by the EPSRC (EP/S515085/1 and EP/L015579/1). We acknowledge support from the Thomas Young Centre under Grant No. TYC-101.

-
- [1] J. G. Bednorz and K. A. Müller, Possible high T_c superconductivity in Ba-La-Cu-O system, *Z. Phys. B: Condens. Matter* **64**, 189 (1986).
- [2] E. Berg, E. Fradkin, S. A. Kivelson, and J. M. Tranquada, Striped superconductors: How spin, charge and superconducting orders intertwine in the cuprates, *New J. Phys.* **11**, 115004 (2009).
- [3] A. Bussmann-Holder and H. Keller, High-temperature superconductors: Underlying physics and applications, *Z. Naturforsch., B: J. Chem. Sci.* **75**, 3 (2020).
- [4] S. I. Uchida, Ubiquitous charge order correlations in high-temperature superconducting cuprates, *J. Phys. Soc. Jpn.* **90**, 111001 (2021).
- [5] B. Keimer, S. A. Kivelson, M. R. Norman, S. Uchida, and J. Zaanen, From quantum matter to high-temperature superconductivity in copper oxides, *Nature (London)* **518**, 179 (2015).
- [6] J. M. Tranquada, Cuprate superconductors as viewed through a striped lens, *Adv. Phys.* **69**, 437 (2020).
- [7] J. M. Tranquada, M. P. M. Dean, and Q. Li, Superconductivity from charge order in cuprates, *J. Phys. Soc. Jpn.* **90**, 111002 (2021).
- [8] D. Fausti, R. I. Tobey, N. Dean, S. Kaiser, A. Dienst, M. C. Hoffmann, S. Pyon, T. Takayama, H. Takagi, and A. Cavalleri, Light-induced superconductivity in a stripe-ordered cuprate, *Science* **331**, 189 (2011).
- [9] M. Hücker, M. V. Zimmermann, G. D. Gu, Z. J. Xu, J. S. Wen, G. Xu, H. J. Kang, A. Zheludev, and J. M. Tranquada, Stripe order in superconducting $\text{La}_{2-x}\text{Ba}_x\text{CuO}_4$ ($0.095 \leq x \leq 0.155$), *Phys. Rev. B* **83**, 104506 (2011).
- [10] J. D. Axe and M. K. Crawford, Structural instabilities in lanthanum cuprate, *J. Low Temp. Phys.* **95**, 271 (1994).
- [11] J. D. Axe, A. H. Moudden, D. Hohlwein, D. E. Cox, K. M. Mohanty, A. R. Moodenbaugh, and Y. Xu, Structural Phase Transformations and Superconductivity in $\text{La}_{2-x}\text{Ba}_x\text{CuO}_4$, *Phys. Rev. Lett.* **62**, 2751 (1989).
- [12] Y.-J. Kim, G. D. Gu, T. Gog, and D. Casa, X-ray scattering study of charge density waves in $\text{La}_{2-x}\text{Ba}_x\text{CuO}_4$, *Phys. Rev. B* **77**, 064520 (2008).
- [13] J. M. Tranquada, J. D. Axe, N. Ichikawa, A. R. Moodenbaugh, Y. Nakamura, and S. Uchida, Coexistence of, and Competition Between, Superconductivity and Charge-Stripe Order in $\text{La}_{1.6-x}\text{Nd}_{0.4}\text{Sr}_x\text{CuO}_4$, *Phys. Rev. Lett.* **78**, 338 (1997).
- [14] A. R. Moodenbaugh, L. Wu, Y. Zhu, L. H. Lewis, and D. E. Cox, High-resolution x-ray diffraction study of $\text{La}_{1.88-y}\text{Sr}_{0.12}\text{Nd}_y\text{CuO}_4$, *Phys. Rev. B* **58**, 9549 (1998).

- [15] E. Berg, E. Fradkin, E. A. Kim, S. A. Kivelson, V. Oganesyan, J. M. Tranquada, and S. C. Zhang, Dynamical Layer Decoupling in a Stripe-Ordered High- T_c Superconductor, *Phys. Rev. Lett.* **99**, 127003 (2007).
- [16] T. Suzuki and T. Fujita, Structural phase transition in $(\text{La}_{1-x}\text{Ba}_x)_2\text{CuO}_{4-\delta}$, *Phys. C (Amsterdam)* **159**, 111 (1989).
- [17] D. E. Cox, P. Zolliker, J. D. Axe, A. H. Moudden, A. R. Moodenbaugh, and Y. Xu, Structural studies of $\text{La}_{2-x}\text{Ba}_x\text{CuO}_4$ between 11–293 K, *MRS Online Proc. Libr.* **156**, 141 (1989).
- [18] S. Barišić and J. Zelenko, Electron mechanism for the structural phase transitions in $\text{La}_{2-x}\text{Ba}_x\text{CuO}_4$, *Solid State Commun.* **74**, 367 (1990).
- [19] S. Sakita, F. Nakamura, T. Suzuki, and T. Fujita, Structural transitions and localization in $\text{La}_{2-x-y}\text{Nd}_y\text{Sr}_x\text{CuO}_4$ with $p \sim 1/8$, *J. Phys. Soc. Jpn.* **68**, 2755 (1999).
- [20] W. E. Pickett, R. E. Cohen, and H. Krakauer, Lattice Instabilities, Isotope Effect, and High- T_c Superconductivity in $\text{La}_{2-x}\text{Ba}_x\text{CuO}_4$, *Phys. Rev. Lett.* **67**, 228 (1991).
- [21] M. Hücker, Structural aspects of materials with static stripe order, *Phys. C (Amsterdam)* **481**, 3 (2012).
- [22] Y. Y. Xue, P. H. Hor, R. L. Meng, Y. K. Tao, Y. Y. Sun, Z. J. Huang, L. Gao, and C. W. Chu, Structural stability and doping in R_2CuO_4 (R = rare-earth), *Phys. C (Amsterdam)* **165**, 357 (1990).
- [23] M. Sera, M. Maki, M. Hiroi, N. Kobayashi, T. Suzuki, and T. Fukase, Thermal conductivity and structural instability in La- and Cu-site-substituted La_2CuO_4 , *Phys. Rev. B* **52**, R735 (1995).
- [24] J. P. Attfield, ‘A’ cation control of perovskite properties, *Cryst. Eng.* **5**, 427 (2002).
- [25] S. J. L. Billinge, G. H. Kwei, and H. Takagi, Structural ground-state of La_2CuO_4 in the LTO phase: Evidence of local disorder, *Phys. C (Amsterdam)* **235-240**, 1281 (1994).
- [26] M. Reehuis, C. Ulrich, K. Prokeš, A. Gozar, G. Blumberg, S. Komiyama, Y. Ando, P. Pattison, and B. Keimer, Crystal structure and high-field magnetism of La_2CuO_4 , *Phys. Rev. B* **73**, 144513 (2006).
- [27] A. Sapkota, T. C. Sterling, P. M. Lozano, Y. Li, H. Cao, V. O. Garlea, D. Reznik, Q. Li, I. A. Zaliznyak, G. D. Gu, and J. M. Tranquada, Reinvestigation of crystal symmetry and fluctuations in La_2CuO_4 , *Phys. Rev. B* **104**, 014304 (2021).
- [28] R. D. Shannon, Revised effective ionic radii and systematic studies of interatomic distances in halides and chalcogenides, *Acta Crystallogr., Sect. A: Cryst. Phys., Diffr., Theor. Gen. Crystallogr.* **A32**, 751 (1976).
- [29] A. A. Coelho, *TOPAS* and *TOPAS-Academic*: An optimization program integrating computer algebra and crystallographic objects written in C++, *J. Appl. Crystallogr.* **51**, 210 (2018).
- [30] B. J. Campbell, J. S. O. Evans, F. Perselli, and H. T. Stokes, Rietveld refinement of structural distortion-mode amplitudes, *IUCr Comput. Comm. Newsl.* **8**, 81 (2007).
- [31] B. J. Campbell, H. T. Stokes, D. E. Tanner, and D. M. Hatch, *ISODISPLACE*: a web-based tool for exploring structural distortions, *J. Appl. Crystallogr.* **39**, 607 (2006).
- [32] P. W. Stephens, Phenomenological model of anisotropic peak broadening in powder diffraction, *J. Appl. Crystallogr.* **32**, 281 (1999).
- [33] See Supplemental Material at <http://link.aps.org/supplemental/10.1103/PhysRevB.106.085112> for further details of the Rietveld refinements and DFT calculations.
- [34] H. T. Stokes, D. M. Hatch, and B. J. Campbell, *ISODISTORT, ISOTROPY* Software Suite, <https://iso.byu.edu/iso/isotropy.php>.
- [35] M. Braden, P. Schweiss, G. Heger, W. Reichardt, Z. Fisk, K. Gamayunov, I. Tanaka, and H. Kojima, Relation between structure and doping in $\text{La}_{2-x}\text{Sr}_x\text{CuO}_{4+\delta}$ a neutron diffraction study on single crystals, *Phys. C (Amsterdam)* **223**, 396 (1994).
- [36] P. Giannozzi, S. Baroni, N. Bonini, M. Calandra, R. Car, C. Cavazzoni, D. Ceresoli, G. L. Chiarotti, M. Cococcioni, I. Dabo, A. D. Corso, S. de Gironcoli, S. Fabris, G. Fratesi, R. Gebauer, U. Gerstmann, C. Gougoussis, A. Kokalj, M. Lazzeri, L. Martin-Samos *et al.*, QUANTUM ESPRESSO: A modular and open-source software project for quantum simulations of materials, *J. Phys.: Condens. Matter* **21**, 395502 (2009).
- [37] P. Giannozzi, O. Andreussi, T. Brumme, O. Bunau, M. B. Nardelli, M. Calandra, R. Car, C. Cavazzoni, D. Ceresoli, M. Cococcioni, N. Colonna, I. Carnimeo, A. D. Corso, S. de Gironcoli, P. Delugas, R. A. DiStasio, A. Ferretti, A. Floris, G. Fratesi, G. Fugallo *et al.*, Advanced capabilities for materials modelling with QUANTUM ESPRESSO, *J. Phys.: Condens. Matter* **29**, 465901 (2017).
- [38] J. P. Perdew, A. Ruzsinszky, G. I. Csonka, O. A. Vydrov, G. E. Scuseria, L. A. Constantin, X. Zhou, and K. Burke, Restoring the Density-Gradient Expansion for Exchange in Solids and Surfaces, *Phys. Rev. Lett.* **100**, 136406 (2008).
- [39] K. F. Garrity, J. W. Bennett, K. M. Rabe, and D. Vanderbilt, Pseudopotentials for high-throughput DFT calculations, *Comput. Mater. Sci.* **81**, 446 (2014).
- [40] M. Cococcioni and S. de Gironcoli, Linear response approach to the calculation of the effective interaction parameters in the LDA + U method, *Phys. Rev. B* **71**, 035105 (2005).
- [41] J. D. Jorgensen, H. B. Schüttler, D. G. Hinks, D. W. Capone II, K. Zhang, M. B. Brodsky, and D. J. Scalapino, Lattice Instability and High- T_c Superconductivity in $\text{La}_{2-x}\text{Ba}_x\text{CuO}_4$, *Phys. Rev. Lett.* **58**, 1024 (1987).
- [42] C. Ablitt, S. Craddock, M. S. Senn, A. A. Mostofi, and N. C. Bristowe, The origin of uniaxial negative thermal expansion in layered perovskites, *npj Comput. Mater.* **3**, 44 (2017).
- [43] S. Pesant and M. Côté, DFT+U study of magnetic order in doped La_2CuO_4 crystals, *Phys. Rev. B* **84**, 085104 (2011).
- [44] T. C. Sterling and D. Reznik, Effect of the electronic charge gap on LO bond-stretching phonons undoped La_2CuO_4 calculated using LDA+U, *Phys. Rev. B* **104**, 134311 (2021).
- [45] J. W. Furness, Y. Zhang, C. Lane, I. G. Buda, B. Barbiellini, R. S. Markiewicz, A. Bansil, and J. Sun, An accurate first-principles treatment of doping-dependent electronic structure of high-temperature cuprate superconductors, *Commun. Phys.* **1**, 11 (2018).
- [46] https://figshare.com/projects/Structure_behaviour_of_La2MgO4/127109.